Raman-spectroscopy investigations of photoinduced changes of the spatial charge-carrier distribution in *p*-type modulation-doped quantum-well structures

R. Hartmann,* J. Kraus, and G. Schaack
Physikalisches Institut der Universität Würzburg, Am Hubland, D-97074 Würzburg, Germany

K. Panzlaff†
Abt. Optoelektronik der Universität Ulm, Oberer Eselsberg, D-89069 Ulm, Germany

(Received 21 June 1996)

We have investigated the consequences of photoinduced changes of the spatial distribution of charge carriers in *p*-type modulation-doped GaAs/$Al_xGa_{1-x}As$–multiple-quantum-well structures on the Raman spectra of hole intersubband excitations as well as of electronic excitations with energies below the smallest quantum-well subband spacings, called low-energy excitations (LEEX). The dynamical process of the hole redistribution after pulsed illumination became obvious in variations of the position, intensity, and line shape of the Raman signals as a function of the delay time between sample illumination and signal detection. The observed modifications of the hole intersubband transitions are due to changes of the width of the single-particle spectrum and of the strength of many-particle interaction effects as well as due to a reduced Coulomb scattering by ionized impurity atoms in the barriers. Referring to the LEEX signals a scattering process is proposed which involves transitions between quantized states in the center regions of the barriers. [S0163-1829(96)00548-6]

I. INTRODUCTION

Superlattices and heterojunctions of alternating semiconducting layers have been attracting considerable attention over the past years because of their unique possibilities for optical and electrical devices. The fabrication of those high-quality semiconductor systems with nearly perfect two-dimensional characteristics has been made possible by the development of crystal-growth techniques such as molecular-beam epitaxy or metal-organic chemical vapor deposition.

In view of a scientific investigation and characterization of both the electronic and phonon states of those structures inelastic light scattering (Raman scattering) experiments have been proven to be a powerful tool with high spatial and spectral resolution. Due to its sensitivity electronic Raman scattering on two-dimensional systems, stimulated by a proposal of Burstein, Pinczuk, and Buchner[1] and successfully performed on an inversion layer of a GaAs/$Al_xGa_{1-x}As$ interface by Abstreiter and Ploog,[2] provides rich information about the electronic energy levels and band structures. Taking advantage of polarization selection rules the investigation of intersubband transitions by inelastic light scattering on a two-dimensional carrier gas also represents a suitable method of separating the different many-particle interaction mechanisms of charge-density excitations (CDE, polarized spectrum) and spin-density excitations (SDE, depolarized spectrum).[3–9] Both types of excitations are subject to the exchange terms of the Coulomb interaction while the CDE's are additionally affected by the direct term of the Coulomb interaction. The resulting energy shift between the intersubband signals of polarized and depolarized Raman spectra is referred to as depolarization shift and is direct evidence of the macroscopic electric field (depolarization field) associated with the induced charge-density fluctuations.[10,11] As a consequence of the many-particle interactions the collective CDE's and SDE's are shifted to energies different from the bare quantum-well subband spacings which correspond to the spectra of single-particle excitations (SPE's).

Because of the strong nonparabolicities of the valence subbands the spectrum of SPE's in *p*-type modulation-doped quantum-well structures is represented by a continuum with finite width and the collective intersubband excitations are strongly Landau damped.[12,13] Therefore the collective effects are efficiently suppressed and the hole intersubband excitations observed in the polarized and depolarized spectra have a dominating single-particle character. This is quite in contrast to the much simpler case of electronic transitions between the parabolic conduction subbands which are characterized by energy spacings independent from the in-plane wave vector $k_\parallel$. The dependence of the position and line shape of the intersubband signals of the quantum-well hole gas from the charge-carrier concentration[14,15] originates both from the changes of the continuum of the SPE and the changes of the strength of collective effects.

In the present work we have concentrated on nonequilibrium effects of CDE and SDE after the production of additional charge carriers by pulsed radiation. In our experimental setup we took advantage of the possibility to reduce the two-dimensional carrier gas density in the wells of modulation-doped heterostructures by illuminating (pump laser) the sample with photons having energies above the barrier band gap.[16,17] Depending on the sample geometry (especially on the spacer thickness) relaxation times of effects due to the pulsed illumination of some milliseconds could be observed at low temperatures.[18] To perform a Raman spectroscopic investigation of the consequences, and the dynamics of the photoinduced changes of the spatial carrier distribution we used a tunable dye laser (probe laser) with photon energies below the barrier band gap and in resonance with

transitions between valence- and conduction-subband states in the quantum wells. In these experiments the sample illumination with the pump laser alternated in time with the detection of the Raman signal. This was realized by a conventional chopper technique with millisecond time resolution described in detail in Ref. 18. Since the actual carrier density in the wells changes with the mean delay time Δt between the pulsed illumination and the detection of the Raman signal,[18] measurements of the Raman excitations depending on the hole gas density could simply be done by changing the chopper frequency. To control the variations of the two-dimensional charge-carrier density we measured the energy of the fundamental quantum-well luminescence,[18] which is conditioned by the many-particle effect of band-gap renormalization (BGR).[16–23]

In the following, we present our results of the illumination effect on hole-intersubband excitations and on low-energy excitations[24,25] (LEEX's) of hitherto unknown origin carried out on *p*-modulation-doped multiple-quantum-well structures. The Δt-dependent variations of the peak positions, linewidths and intensities of the hole intersubband transitions are discussed in terms of the width of single-particle spectrum, the influence of Coulomb scattering by the normally ionized impurity atoms in the barriers as well as in terms of the strength of many-particle interaction effects. Referring to the LEEX signals our experimental results give good arguments for an interpretation as intersubband excitations of photoinduced holes in the potential minima in the centers of the barriers. The variations of their peak positions and intensities with the density of the photoinduced holes in the barriers are discussed and a Raman-scattering process is proposed.

II. EXPERIMENTAL DETAILS

Our experiments were performed on *p*-type modulation-doped GaAs/$Al_xGa_{1-x}As$ multiple-quantum-well structures grown by molecular-beam epitaxy. The sample that will be discussed in detail in the following consists of 10 periods of 11-nm-wide GaAs wells, separated by 24.5-nm-wide spacers from the 15-nm-wide Be-doped layers (doping concentration $n_{Be}=3\times10^{17}$ cm^{-3}) in the centers of the $Al_{0.32}Ga_{0.68}As$ barriers. From Raman spectroscopic measurements performed on a similar sample under nearly the same experimental conditions (temperature, laser power density) as realized in our present measurements we derived a hole density of $p=1.7\times10^{11}$ cm^{-2} ($T=2$ K, sample in the dark).[13] Due to this quasi-two-dimensional hole concentration in our sample only the lowest heavy-hole quantum-well subband h_0 is occupied with holes in the region $0\leqslant k_\parallel\leqslant k_F$ of the k space and therefore may serve as an initial state for hole transitions to higher valence subbands.

The samples were immersed in superfluid liquid helium ($T=2$ K) in a bath cryostat or in a split coil superconducting magnet system. The Raman measurements were carried out in backscattering configuration with vanishing in-plane wave-vector transfer. The scattering geometry is described in the standard notation $z(e_i,e_s)-z$, where e_i and e_s mean the polarization of the incident and scattered light, respectively, and z ($-z$) is the wave-vector direction of the incident (scattered) radiation parallel to the sample growth direction. An Ar^+ laser-pumped cw dye laser (Pyridine, probe laser) emitting photons with energies below the barrier band gap was used to study hole intersubband excitations under resonance conditions. The scattered light was dispersed with a triple spectrograph (Dilor XY) and analyzed by an optical multichannel detector. The photoinduced reduction of the carrier concentrations in the quantum wells by sample illumination with photons of energies far above the barrier band gap was achieved by using the 514-nm line of an Ar^+ laser (pump laser). A chopper separated the sample illumination by the pump laser from the detection of the inelastically scattered probe-laser photons.[18] The mean delay time Δt defined as the period between the end of the sample illumination t_{pump} and the middle of the detection time $t_{detection}$ (see Fig. 1 in Ref. 18) could be varied by changing the rotation frequency of the chopper wheel. Since the actual carrier density in the wells depends on Δt our experimental setup enabled us to study quantitatively the effects of a variation of the hole gas density on Raman excitations under conditions of a fixed experimental geometry. Delay times Δt between approximately 0.3 and 200 ms could be attained. Spectra measured at $\Delta t=0$ ms show a very strong luminescence background. Spectra of this type are not considered in our discussion. Because of the weakness of Raman signals $t_{detection}$ had to be chosen large enough for a reasonable signal-to-noise ratio at the expense of losing gradually the clear definition of Δt. The duty cycle ($t_{detection}$ or t_{pump} divided by the repetition time) was $\approx$50% for the Raman detection and $\approx$20% for the pump laser. The typical power density of the probe laser is 15 mW/cm^2 and of the pump laser below 200 mW/cm^2 in order to avoid sample heating.

To control the variations of the carrier density in the quantum wells we measured the energy of the luminescence from the wells, which is conditioned by the many-particle effect of band-gap renormalization (BGR).[16–23] Results of theoretical investigations of the BGR (Ref. 19) [formula (1) of Ref. 18] provide us with an approximate value for the variation Δp of the quantum-well hole density. More details about the method as well as its limitations are described in Ref. 18.

III. HOLE INTERSUBBAND EXCITATIONS

The Raman spectra observed in $z(x,x)-z$ geometry (polarized spectrum) for different delay times Δt with a dye laser energy of 13 144 cm^{-1}, i.e., close to but slightly below the resonance energy of 13 180 cm^{-1}, due to hole transitions from the occupied subband h_0 to the first excited heavy-hole subband h_1 are given in Fig. 1. The spectrum without using the pump laser is equivalent to a delay time $\Delta t=\infty$ in our experiment.

Depending on Δt, the shape of the Raman line is affected by the pump illumination with respect to peak height, half width, and energy. Short delay times Δt result in a more pronounced signal of the transition $h_0\rightarrow h_1$ due to an increase of the peak height and a decrease of the half width. In addition the peak position weakly shifts to lower energies.

We attribute this delay-time-dependent effects on $h_0\rightarrow h_1$ transitions to photoinduced changes of the spatial distribution of the holes within the sample. It is known that photons with energies above the barrier band gaps of modulation-

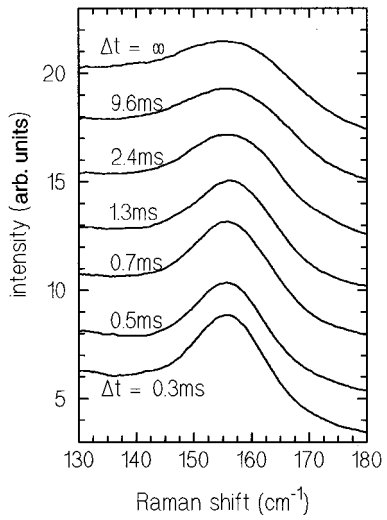

FIG. 1. Polarized Raman spectra of the hole intersubband transition $h_0 \rightarrow h_1$ observed for different delay times Δt. The dye laser beam has an energy of 13 144 cm^{-1} and a power density of 15(W/cm^2).

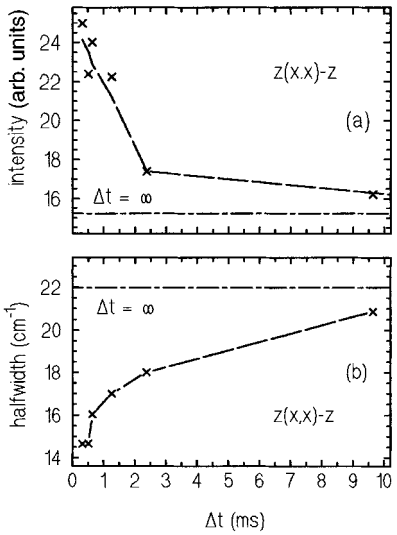

FIG. 2. Fitting results of the $h_0 \rightarrow h_1$ intersubband excitations of Fig. 1 as a function of the delay time Δt showing the strong impact of the Ar^+ laser illumination on the peak height (a) and the half width (b) of the Raman signals. The horizontal dashed lines represent the peak height, respectively, half width for $\Delta t = \infty$; i.e., no Ar^+ laser is used in this case. The time-dependent variations clearly correspond to the degree of the reduction of the hole density Δp in the quantum wells (Fig. 4 of Ref. 18).

doped heterostructures efficiently reduce the free-charge-carrier densities in the wells. According to the model described in Refs. 16, 17 (see also Ref. 18 and its Fig. 3), the electron-hole pairs created in the barriers by the Ar^+ laser light are separated by the built-in electric field: The electrons move into the quantum wells reducing the density of the hole gas by recombination, while the photoinduced holes are attracted by the ionized acceptor atoms in the doped barrier layers. To reachieve the equilibrium conditions the barrier holes finally return to the wells by a tunneling process through the spacer regions. This dynamical process of hole tunneling is observable with our simple chopper technique due to the finite lifetime of the photoexcited holes in the potential minimum of the barrier center region.[18] The variation of the position of the fundamental quantum-well luminescence as a function of Δt (inset in Fig. 2 of Ref. 18) is direct evidence of the reduction of the charge-carrier density in the quantum wells and a consequence of the many-body effect of BGR. Neglecting the charge-density dependence of the strength of excitonic interactions, which is taken into account in Ref. 18, and interpreting the shift of the fundamental quantum-well luminescence signal only as an effect of the BGR, the determination of the shift of the peak position enables us to estimate the variation of the hole density p in the quantum wells by using the expression of Kleinman and Miller[19] as described in Ref. 18. In Fig. 4 of Ref. 18 the calculated variation Δp of the hole concentration is displayed versus the mean delay time Δt.

In Figs. 2 and 3 the peak height, half width, and Raman shift of the $h_0 \rightarrow h_1$ intersubband transition obtained by fitting sums of Gaussian and Lorentzian curves are plotted versus Δt. With increasing Δt the values for the peak height, halfwidth, and peak position gradually approach the corresponding values for $\Delta t = \infty$. A comparison between the delay-time-dependent change of the hole density (Fig. 4 of Ref. 18) and the modifications of the line-shape parameters of the hole intersubband transition $h_0 \rightarrow h_1$ gives strong proof of a charge-density-induced effect.

Because of the strong nonparabolicities of the valence subbands and the resulting dependence of the hole subband spacings on the in-plane wave vector $k_\parallel$, the single-particle spectrum of hole intersubband excitations is a continuum of transitions of different energies. This is in contrast to the nearly parabolic conduction subbands with constant separations. Figure 4 shows the calculated valence-subband structure of the sample studied here including the position of the Fermi wave vector $[k_F(p) = \sqrt{2\pi p}]$ assuming a hole concentration[13] of $p = 1.7 \times 10^{11}$ cm^{-2}. The vertical arrows symbolize the dipole-allowed hole transitions in the region $0 < k_\parallel \leq k_F(p)$ which contribute to the spectrum of the intersubband excitations $h_0 \rightarrow h_1$. Their contributions to the measured Raman signals depend on the probe-laser energy, the

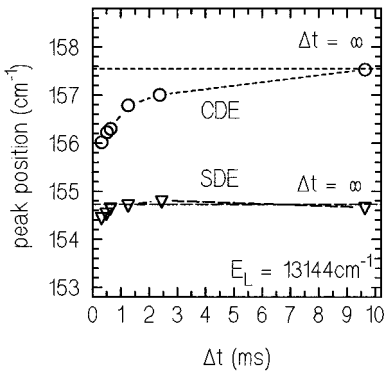

FIG. 3. Variation of the photoinduced shift of the intersubband transition energy in the polarized (CDE) and depolarized (SDE) Raman spectra with delay time Δt (laser energy $E_L = 13\,144$ cm^{-1}). The horizontal dashed lines represent the excitation energies for $\Delta t = \infty$, respectively.

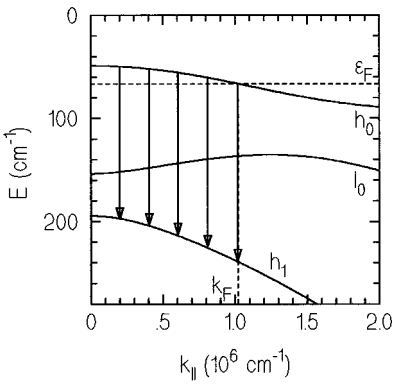

FIG. 4. Continuum of possible contributions to the single-particle spectrum of intersubband excitations $h_0 \rightarrow h_1$ in p-doped quantum wells. The finite width of the continuum depends on the carrier density p in the well which determines the size of the Fermi wave vector $k_F(p)$. The given value of k_F corresponds to an assumed hole concentration $p = 1.7 \times 10^{11}$ cm^{-2}.

densities of states, and the transition probabilities.[26,27] Since the finite width of the single-particle continuum is given by the value of $k_F(p)$, the above-barrier band-gap illumination decreases the Fermi wave vector $k_F(p)$ and hence the width of the transition continuum resulting in a shrinkage of the half width. The back transfer of the barrier holes into the wells after the sample illumination brings an extension of the region of possible hole transitions $h_0 \rightarrow h_1$ in k space by increasing $k_F(p)$ in accordance with our experimental results [Fig. 2(b)].

The delay-time Δt-related shift of the hole intersubband transition (Fig. 3) is also influenced by the change of the width of the continuum of SPE's. As it follows directly from the subband structure of Fig. 4, a reduction of the quantum-well carrier density, i.e., a decrease of $k_F(p)$, cancels the possible scattering paths with highest transition energies between the subbands h_0 and h_1, i.e., the depopulation of the wells causes a decrease of the peak position of the Raman signal. The gradual back transfer of the holes reincreases $k_F(p)$ and allows scattering events of growing excitation energies.

Besides the subband structure the line shape of intersubband excitations is also affected by wave-vector relaxation processes due to the Coulomb potential of the ionized impurities in the barrier regions.[28] The efficiency of the impurity-induced scattering can be suppressed either by an extension of the widths of the spacer layers[28] or by a photoinduced compensation, respectively, screening of the ionized impurity atoms.[29,30] In our experiments the photocreated barrier holes weaken the influence of the structural defects on the light-scattering process and therefore enlarge the contribution of vertical intersubband transitions in the k space to the Raman signal. With increasing delay time Δt the nonvertical electronic transitions with violation of the momentum conservation reincreases due to the impurity-induced Coulomb scattering. This also contributes to the observed variations of the peak height and half width of the excitation line $h_0 \rightarrow h_1$ (Fig. 2). Our assumption of a pronounced influence of the barrier ions on the signals of intersubband excitations in the quantum wells is supported by the observation that the integral intensity of the $h_0 \rightarrow h_1$ transition ($\approx$peak height$\times$half width) is almost unaffected by the sample illumination (Fig. 1) although the shrinkage of the single-particle continuum reduces the filling of the initial subband state h_0.

So far we have interpreted the observed photoinduced effects on the shape and position of the intersubband excitation $h_0 \rightarrow h_1$ in terms of variations of the single-particle continuum and of carrier scattering by ionized impurities, but without considering the many-particle effects of collective transitions which originate in the Coulomb coupling of isoenergetic SPE's. The energies of the collective transitions are shifted from the positions of the single-particle modes due to a coupling mechanism of the charge carriers by direct and exchange Coulomb interaction.[3–9] SDE's observed in depolarized spectra $[z(xy)-z]$ are shifted to lower energies compared to SPE's due to the exchange term of the Coulomb interaction. On the other hand, the polarized spectra $[z(xx)-z]$ of CDE's are observed with shifts towards higher energies due to the consequences of the direct and indirect Coulomb interaction. Because of the complex valence-band structure the number of isoenergetic SPE's is limited for p-doped systems, i.e., many-particle effects are strongly suppressed for two-dimensional hole gases.[13] In addition the finite width of the single-particle continuum even for vanishing momentum transfer $k_\parallel = 0$ enhances the occurrence of Landau damping[12] of the collective excitations.

The energies of CDE's and SDE's at zero wave vector can be written as[31]

$$\hbar\Omega_{\mathrm{CDE}}(0) = (\varepsilon_1 - \varepsilon_0) + \left(V_c(0) - \frac{1}{2} V_e(0) \right)(p_0 - p_1) = \hbar\Omega_{01} + \alpha_{01} - \beta_{01}, \tag{1}$$

$$\hbar\Omega_{\mathrm{SDE}}(0) = (\varepsilon_1 - \varepsilon_0) - \frac{1}{2} V_e(0)(p_0 - p_1) = \hbar\Omega_{01} - \beta_{01}, \tag{2}$$

where V_c and V_e are Coulomb and exchange interaction, respectively. Changing the hole concentration in the quantum wells a shift of the peak position of the CDE's and SDE's can occur due to variations of the single-particle continuum determined by $k_F(p_0)$ as well as by variations of the collective shifts depending on the difference in the population densities $p_0 - p_1$ of the subbands taking part on the hole transitions.

The effects of above-barrier band-gap illumination on the spectra of CDE and SDE concerning the peak position of the hole excitation $h_0 \rightarrow h_1$ are given in the plot of Fig. 3. The depopulation of the quantum-wells results in an energy shift of the CDE, which is about 4 times larger than the corresponding energy shift of the SDE. This difference is caused by the fact that the charge-density-dependent effects on the variation of the single-particle continuum width and on the exchange term of the many-particle interaction partly compensate each other in the case of the depolarized spectra of SDE, while the direct Coulomb interaction valid in the case of CDE supports the shift of the peak position of the SPE spectrum. The decrease of the Raman shift of SDE at additional illumination can be seen as an indication for a dominating single-particle character of the intersubband excitation and gives evidence for a weak exchange Coulomb interaction of the holes in GaAs.

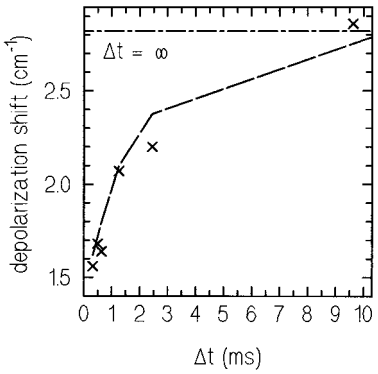

FIG. 5. Depolarization shift between the CDE and SDE of the $h_0 \rightarrow h_1$ transition measured with the laser energy $E_L = 13\,144$ cm^{-1}. The refilling of the quantum wells after the sample illumination can be observed by the increase of the energetic shift.

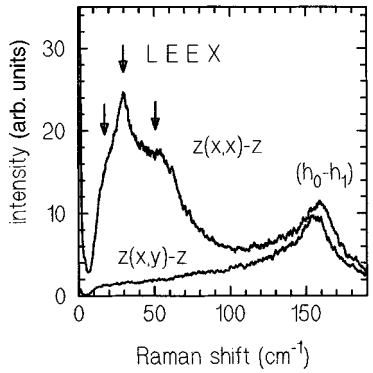

FIG. 6. Polarized and depolarized spectrum of the p-doped GaAs/Al$_x$Ga$_{1-x}$As multiple-quantum-well structure observed with a laser energy $E_L = 13\,164$ cm^{-1}. In the polarized spectrum the Raman signals of the low-energy excitations (LEEX) can be seen.

Even though the collective effects are found to be weak for p-type modulation-doped heterostructures because of the nonparabolic valence subbands they can be observed clearly due to the term α_{01} of Eq. (1) by comparing the peak positions in the polarized and depolarized Raman spectra. Figure 5 reveals the time-dependent differences in the Raman shifts of CDE and SDE as being measured in both scattering geometries under otherwise identical conditions. This energy difference, in the literature usually referred to as depolarization shift, is small for short delay times Δt and steadily increases with time, approaching the value for the maximum hole densities in the wells. The refilling of the quantum wells after illumination increases the energetic difference between CDE and SDE, which is formally reflected by an increasing value for α_{01} in Eq. (1) and referred to as an increase of the depolarization field.[10,11] Analogous experiments were carried out for different probe-laser energies as well as on a one-sided modulation-doped single-quantum-well structure with results corresponding satisfyingly to those described above.

IV. LOW-ENERGY EXCITATIONS (LEEX's)

The LEEX's,[24] excitations of hitherto unknown origin, can be observed in the polarized spectra of p-type modulation-doped multiple quantum wells. Several peaks can be resolved with Raman shifts smaller than 60 cm^{-1}, i.e., below the energies of hole intersubband excitations. Because of their low energies these excitations cannot be explained by conventional electronic transitions between the quantized quantum-well states. Since they do not show a significant dependence on the in-plane component of the scattering wave-vector[24,25] LEEX's are not multilayer plasmons of the type observed in n-type superlattices[32] either. Raman-scattering experiments with a magnetic field applied parallel and perpendicular to the growth direction of the sample indicate the quasi-two-dimensional character of the LEEX's.[24] Additional measurements by Pinczuk *et al.*[24,25] indicate a dependence of the Raman shifts and half widths from the hole gas concentration. Figure 6 shows that LEEX's are visible in the polarized spectrum only, but not in the depolarized spectrum under otherwise the same conditions. In the following the complex spectrum of the LEEX's will be interpreted as a superposition of three components with excitation energies of approximately 55, 30, and 20 cm^{-1}. The mode at 160 cm^{-1} in Fig. 6 represents the hole intersubband excitation $h_0 \rightarrow h_1$ discussed in Sec. III.

The effect of the above-barrier band-gap illumination on the LEEX spectrum is shown in Fig. 7 for different delay times Δt. With decreasing Δt, i.e., with an increasing number of photoexcited holes in the potential minima in the centers of the Al$_x$Ga$_{1-x}$As barriers the efficiency of the LEEX scattering process increases. Simultaneously the observed Raman shifts become smaller by the hole transfer into the barriers.

We interpret the LEEX's as intersubband transitions of photoinduced holes with a density $-\Delta p$ (Fig. 4 in Ref. 18) in the potential minima in the centers of the barriers between neighboring quantum wells [Fig. 12(b)]. Small subband spacings of less than 60 cm^{-1} which correspond well to the peak positions found for the LEEX signals occur due to the weak charge-carrier confinement realized in the flat potential of a quasitriangular shape in the barrier center regions of modulation-doped multiple quantum wells.

Our interpretation is supported by considering the intensities of the LEEX components with Raman shifts of about 55 and 30 cm^{-1} as a function of the mean delay time Δt (Fig. 8). The LEEX structure with an energy of about 20

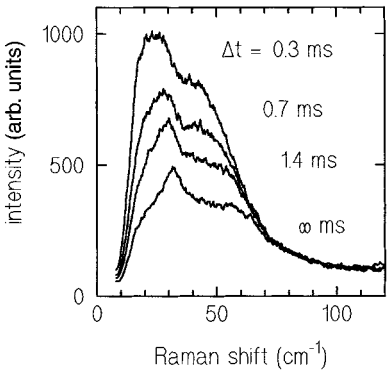

FIG. 7. Effect of the photoinduced change of the spatial distribution of the hole gas on the LEEX structure. With decreasing time delay Δt the efficiency of the scattering by LEEX increases while simultaneously the observed Raman shift becomes smaller.

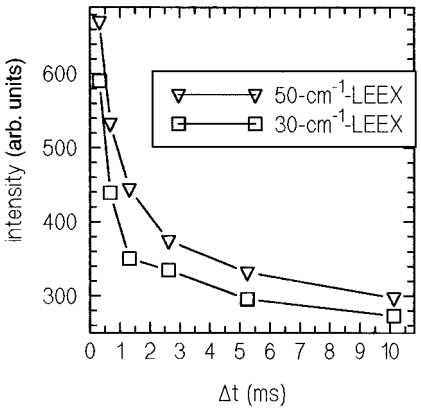

FIG. 8. Intensity of the LEEX components with Raman shifts of approximately 30 and 55 cm^{-1} as a function of Δt. The intensity decreases with increasing relaxation of the photoinduced holes in the barriers according to the decreasing occupation of the lowest subband state in the barrier potential well.

cm^{-1} (Fig. 6) is not displayed in this plot because of the difficulties to fit this weak signal. With increasing Δt the intensities decrease. According to our model this is due to the decrease of the hole density $-\Delta p$ in the barriers, i.e., due to the decreasing occupation of the lowest subband state in the barrier potential.

The increase of the excitation energies of the LEEX's with Δt (Fig. 9) is also well correlated to the variation of the hole density $-\Delta p$ in the barriers. The transfer of quantum-well holes into the Be-doped barrier regions leads to a reduction of the depth of the triangular shape barrier potential, approaching the flat band case, due to a compensation, respectively, neutralization of the ionized acceptors. This results in a shrinkage of the barrier state spacings and thus in

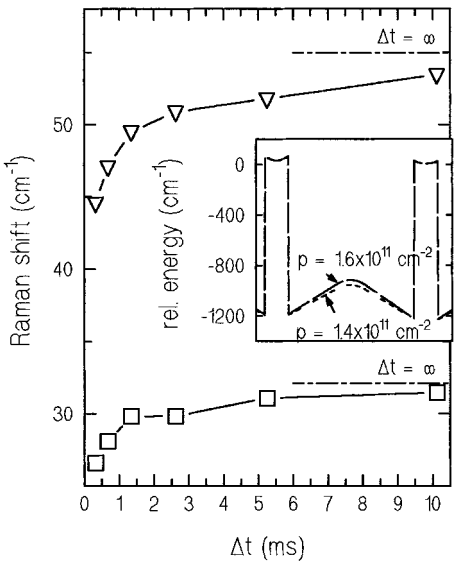

FIG. 9. Illumination effect on the Raman shift of the LEEX's. With decreasing number of photoexcited holes in the barrier potential wells, i.e., with increasing Δt the depth of the confining potential increases (inset) and the subband distances become larger. The inset gives the barrier potential shape calculated for the quantum-well hole densities $p=1.6\times10^{11}$ cm^{-2} and $p=1.4\times10^{11}$ cm^{-2}.

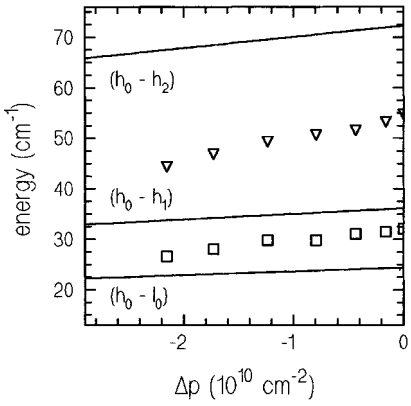

FIG. 10. Experimental excitation energies of the LEEX's and calculated energy spacings between the barrier subbands h_0-l_0, h_0-h_1, and h_0-h_2 as a function of barrier hole density.

the observed decrease of the LEEX energies. With the proceeding relaxation of the charge carriers the number of holes in the barrier potential decreases, i.e., the depth of the confining potential and therefore the subband distances become larger. The consequent increase of the LEEX energies with Δt is demonstrated in the plot of Fig. 9. The inset illustrates the shape of the valence-band edge according to a self-consistent calculation assuming quantum-well hole densities $p=1.6\times10^{11}$ and 1.4×10^{11} cm^{-2}. The charge-density-related band bending is clearly reflected. By describing the center of the barrier potentials by a parabolic shape, we have calculated the energies of the barrier subband states for different numbers of barrier holes easily as eigenvalues of the harmonic oscillator. In Fig. 10 the calculated energy spacings between h_0 and the barrier subbands l_0, h_1, and h_2 are shown as a function of the barrier hole density and compared to our experimental data of LEEX energies which are also displayed as a function of the density of photoinduced holes in the barrier center regions deduced from Fig. 4 of Ref. 18. With respect to our crude assumptions the agreement between the calculated and experimental values (especially the slopes with Δp) is acceptable.

Figure 11 gives the resonance enhancement of the Raman intensities of two LEEX components in comparison with the behavior of the $h_0\rightarrow h_1$ quantum-well transition as a function of the photon energy E_L of the probe-laser beam. The LEEX's and the $h_0\rightarrow h_1$ intersubband transition of the quantum wells appear at laser energies very close to each other. This means that the scattering intensities of the LEEX's show maxima at laser energies which correspond to subband distances in the wells. The intermediate state in the Raman-scattering process of a LEEX is a quantum-well electronic subband state. On the other hand, the resonance maxima of the LEEX components are found slightly shifted to lower energies compared to the resonance peak of the $h_0\rightarrow h_1$ quantum-well transition. With decreasing Raman shifts the resonance maxima of the LEEX's shift to lower energies.

Considering the resonance behavior of the LEEX components, we assume a scattering mechanism in which the intersubband transition within the confining barrier potential is induced by interaction with a quantum-well exciton. In Fig. 12 the proposed mechanism of the LEEX scattering process is schematically shown both in the real and in the reciprocal

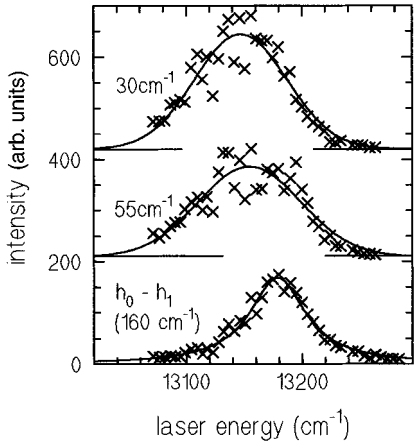

FIG. 11. Resonance behavior of two LEEX components and of the quantum-well hole excitation $h_0 \rightarrow h_1$. The scattering intensities of the LEEX's show maxima at laser energies close to the energy of resonant excitation of the intersubband transition.

space. In this third-order process two optical transitions are associated with intermediate exciton states. The exciton created by the probe-laser beam with appropriate photon energy is assumed to be scattered into a second real exciton state by interaction with a free hole in the barrier center region before it annihilates under emission of a photon. The energy transfer to a hole in the barrier potential is assumed to be mediated by the direct term, i.e., the long-range part of the Coulomb interaction due to the large spatial separation between the centers of the barriers and the quantum wells. This results in the transition of a barrier hole. The strongest resonant enhancements of the LEEX signals are expected if the energy spacing between the quantum-well exciton states involved in the process coincides with the energy separation of the subband states in the barriers. In compliance with the subband structure calculations of Fig. 4 quantum-well subband distances of the magnitude close to the measured LEEX energies occur between the hole bands l_0 and h_1 for in-plane wave vectors in the range of $0\ \mathrm{cm}^{-1} < k_{\parallel} \lesssim 0.4 \times 10^6\ \mathrm{cm}^{-1}$ and between h_0 and l_0 for $k_{\parallel} \approx 1.6\ \mathrm{cm}^{-1}$. Our assumption of an efficient coupling between holes of the wells and the barriers by the direct term of the Coulomb interaction is supported by the experimental result that LEEX's are observed in the polarized spectra only.

Our experimental situation is similar to an experiment on an asymmetric double-quantum-well structure proposed in Ref. 31. According to these studies resonant excitations of the charge carriers in one quantum well are supposed to bring about CDE's, but no SDE's in the neighboring well. It is argued that the direct term of the Coulomb interaction couples charge carriers even in the case of vanishing overlap of the corresponding wave functions, whereas the exchange term of the Coulomb interaction lacks this ability. Since the hole gases in the quantum wells and barrier regions of our sample are spatially separated from each other there exists no coupling due to the exchange Coulomb interaction, but only due to the long-range direct term. Our suggestion of a coupling mechanism between the well and barrier holes, i.e., over a distance more than the nominal spacer thickness $L_z = 245$ Å is reasonable by taking into account the weak confinement of the holes in the barriers resulting from the

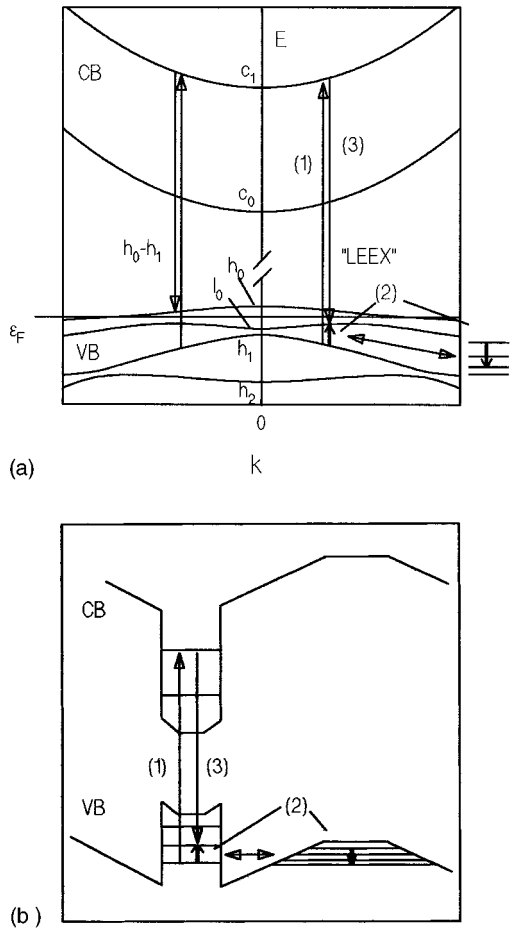

FIG. 12. Illustration of a third-order LEEX scattering process in the real (a) and reciprocal space (b): An exciton created by the incoming probe-laser light (1) changes into another real quantum-well state (2) by simultaneously exciting a barrier hole due to the coupling by direct Coulomb interaction (2). In the following step the quantum-well exciton recombines (3) under emission of a photon. For reasons of clearness the scattering mechanism of the quantum-well hole intersubband transition $h_0 \rightarrow h_1$ is shown as well in (a).

triangular shape of the barrier potential.

To calculate the efficiency of the inelastic light scattering on LEEX's, we assume a third-order scattering mechanism similar to that developed by Danan *et al.*[33] in order to describe the resonance behavior of intersubband excitations in *n*-type one-sided modulation-doped quantum-well structures. The intensity of the resonantly scattered light in this third-order process is given by

$$I \propto \left| \sum_{\nu\nu'} \left(\frac{M^*_{\nu'}(H_e)_{\nu\nu'} M_{\nu}}{(E_{\nu} - \hbar\omega_L + i\eta)(E_{\nu'} - \hbar\omega_{\mathrm{SL}} + i\eta)} \right) + \left(\frac{M^*_{\nu}(H_e)_{\nu'\nu} M_{\nu'}}{(E_{\nu'} - \hbar\omega_L + i\eta)(E_{\nu} - \hbar\omega_{\mathrm{SL}} + i\eta)} \right) \right|^2, \qquad (3)$$

where M_{ν} describes the optical matrix element for the creation of an exciton in a state $|\nu\rangle$ with an energy E_{ν} and $(H_e)_{\nu\nu'}$ the transition of the exciton from a state $|\nu\rangle$ into a state $|\nu'\rangle$. $\hbar\omega_L$ and $\hbar\omega_{\mathrm{SL}}$ are the energies of the incident and

inelastically scattered light, respectively. The phenomenological broadening of the signal is covered by the parameter η. Using this expression and assuming a constant transition-matrix element $(H_e)_{\nu\nu'}$, we calculated the resonance curves of the different LEEX components involving transitions between the valence subbands h_0, l_0, and h_1 and the first excited conduction subband c_1. The positions of the resonance maxima are found to be mainly determined by optical transitions under participation of l_0- and h_1-subband states close to the center of the Brillouin zone. The calculations further reflect the experimental observation that LEEX components with smaller Raman shifts have their resonance positions at lower probe-laser photon energies.

Finally our interpretation of the LEEX's is supported by measurements on a one-sided modulation-doped single quantum well. The potential shape of a one-sided modulation-doped single quantum well does not provide an appropriate charge-carrier confinement in the barrier regions along the growth direction. Therefore quantized barrier states are absent, meaning that LEEX structures cannot occur in the polarized spectra of these samples in agreement with our experimental findings.

V. SUMMARY

In summary, the effects of a hole density reduction in the quantum wells of p-type modulation-doped heterostructures by pulsed above-barrier band-gap illumination on hole intersubband excitations and LEEX's of hitherto unknown origin are presented. Using a simple experimental setup, which allows the variation of the time delay Δt between the quantum-well depopulation and the detection of the Raman signals, measurements of the hole gas density dependence could be performed on one sample under fixed experimental geometry and the dynamical process of the hole relaxation could be investigated by the analysis of the shapes of the Raman spectra. To control the photoinduced variations of the hole distribution in the samples we determined the position of the fundamental quantum-well luminescence.

Referring to the hole intersubband transitions $h_0 \rightarrow h_1$ within the quantum wells the above-barrier band-gap illumination results in a decrease of the Raman shifts and half widths and in an increase of the peak heights of the lines. The time-dependent changes of the signal parameters are related to the actual hole distribution in the samples and were explained by modifications in the single-particle continuum width, variations of the influences of the ionized barrier impurities, and of the strengths of many-particle Coulomb interactions. Although collective effects are only weakly pronounced for hole intersubband excitations due to the complex nonparabolic valence-band structure, they are well present. They can be observed as depolarization shifts between the spectra measured in parallel and perpendicular scattering geometries. The refilling of the wells with increasing delay time Δt strengthens the many-particle effects and gradually increases the depolarization shift.

The transfer of the quantum-well holes into the barrier regions also modifies the Raman signals of the LEEX's occuring in the polarized spectra of p-doped heterostructures at energies close to the Rayleigh line. The time-dependent variations of the energies and intensities of the LEEX's clearly correspond to the changing number of photoexcited holes in the barriers. The small excitation energies as well as the results of our two-laser experiments give evidence for interpreting them as transitions of photoinduced barrier holes between quantized states in the flat confining barrier potential. We assume a scattering mechanism in which the quantum-well exciton created by the incoming probe-laser beam changes into another excitonic state with a transfer of the released energy onto a barrier hole by means of direct Coulomb interaction. As a consequence a hole in the barrier is excited to a higher subband state there and the quantum-well exciton recombines emitting a photon with a Raman shift corresponding to the transferred energy. The experimental observation of LEEX signals with maximum intensities for probe-laser energies providing resonant pumping of excitonic quantum-well states is thus accounted for by our model. The efficiency of this charge-carrier coupling is resonantly enhanced in the case of identical energy spacings between the subband states of the quantum wells and barrier regions being involved in the third-order scattering process. The selection rule for the occurrence of LEEX scattering, i.e., the absence of LEEX's signals in depolarized Raman-spectra results from the disability of exchange interaction in providing a coupling between charge carriers under conditions of nonoverlapping wave functions. The proposed scattering scheme is further supported by the absence of LEEX structures in the spectra measured on asymmetric p-doped single-quantum-well systems due to the missing appropriate confinement of the barrier holes.

ACKNOWLEDGMENTS

We want to thank C. Schüller and T. Friedrich for their helpful calculations of the subband structure and barrier potential bending, respectively. We are also grateful to M. Kirchner and P. Ils, who made available to us some of their experimental results.

*Present address: Paul-Scherrer-Institut, CH-5232 Villigen, Switzerland.

†Present address: ANT Nachrichtentechnick GmbH, Gerberstraβe 33, D-71522 Backnang, Germany.

[1] E. Burstein, A. Pinczuk, and S. Buchner, in *Physics of Semiconductors 1978*, IOP Conf. Proc. No. 43, edited by B. L. H. Wilson (Institute of Physics and Physical Society, London, 1979), p. 1231.

[2] G. Abstreiter and K. Ploog, Phys. Rev. Lett. **42**, 1308 (1979).

[3] M. V. Klein, in *Light Scattering in Solids*, edited by M. Cardona, Topics in Applied Phyics Vol. 8 (Springer, Berlin, 1975), p. 147.

[4] A. Pinczuk, H. L. Störmer, R. Dingle, J. M. Worlock, W. Wiegmann, and A. C. Gossard, Solid State Commun. **32**, 1001 (1979).

[5] A. Pinczuk, J. M. Worlock, H. L. Störmer, R. Dingle, W. Wiegmann, and A. C. Gossard, Solid State Commun. **36**, 43 (1980).

[6] E. Burstein, A. Pinczuk, and D. L. Mills, Surf. Sci. **98**, 451 (1980).

[7] T. Ando, A. B. Fowler, and F. Stern, Rev. Mod. Phys. **54**, 437 (1982).

[8] D. Gammon, B. V. Shanabrook, J. C. Ryan, and D. S. Katzer, Phys. Rev. B **41**, 12 311 (1990).
[9] D. Gammon, B. V. Shanabrook, J. C. Ryan, D. S. Katzer, and M. J. Yang, Phys. Rev. Lett. **68**, 1884 (1992).
[10] W. P. Chen, Y. J. Chen, and E. Burstein, Surf. Sci. **58**, 263 (1976).
[11] D. A. Dahl, and L. J. Sham, Phys. Rev. B **16**, 651 (1977).
[12] C. Schüller, J. Kraus, V. Latussek, and J. K. Ebeling, Solid State Commun. **81**, 3 (1992).
[13] C. Schüller, J. Kraus, G. Schaack, G. Weimann, and K. Panzlaff, Phys. Rev. B **50**, 18 387 (1994).
[14] M. Kirchner, diploma thesis, Universität Würzburg, Germany, 1992.
[15] C. Schüller, Ph.D. thesis, Universität Würzburg, Germany, 1994.
[16] E. A. Meneses, F. Plentz, and C. A. C. Mendonca, Superlatt. Microstruct. **5**, 11 (1989).
[17] A. S. Chaves, A. F. S. Penna, J. M. Worlock, G. Weimann, and W. Schlapp, Surf. Sci. **170**, 618 (1986).
[18] R. Hartmann, J. Kraus, G. Schaack, and K. Panzlaff, Phys. Rev. B **53**, 13 011 (1996).
[19] D. A. Kleinman and R. C. Miller, Phys. Rev. B **32**, 2266 (1985).
[20] S. Schmitt-Rink, D. S. Chemla, and D. A. B. Miller, Phys. Rev. B **32**, 6601 (1985).
[21] M. H. Meynadier, J. Orgonasi, C. Delalande, J. A. Brum, G. Bastard, M. Voos, G. Weimann, and W. Schlapp, Phys. Rev. B **34**, 2482 (1986).
[22] C. Delalande, G. Bastard, J. Orgonasi, J. A. Brum, H. W. Liu, M. Voos, G. Weimann, and W. Schlapp, Phys. Rev. Lett. **59**, 2690 (1987).
[23] C. Weber, C. Klingshirn, D. S. Chemla, D. A. B. Miller, J. E. Cunningham, and C. Ell, Phys. Rev. B **38**, 12 748 (1988).
[24] A. Pinczuk, H. L. Störmer, A. C. Gossard, and W. Wiegmann, in *Proceedings of the 17th International Conference on the Physics of Semiconductors*, edited by J. D. Chadi and W. A. Harrison (Springer, New York, 1985), p. 329.
[25] A. Pinczuk, D. Heiman, R. Sooryakumar, A. C. Gossard, and W. Wiegmann, Surf. Sci. **170**, 573 (1986).
[26] M. Kirchner, C. Schüller, J. Kraus, and G. Schaack, Phys. Rev. B **47**, 9706 (1993).
[27] F. Bechstedt, H. Gerecke, and J. Kraus, Phys. Rev. B **45**, 1672 (1992).
[28] A. Pinczuk, J. M. Worlock, H. L. Störmer, A. C. Gossard, and W. Wiegmann, J. Vac. Sci. Technol. **19**, 561 (1981).
[29] J. Kraus, G. Weimann, and K. Panzlaff, J. Phys. Condens. Matter **7**, 7761 (1995).
[30] G. Ambrazevicius, M. Cardona, R. Merlin, and K. Ploog, Solid State Commun. **65**, 1035 (1988).
[31] Ming Ya Jiang, Solid State Commun. **84**, 81 (1992).
[32] D. Olego, A. Pinczuk, A. C. Gossard, and W. Wiegmann, Phys. Rev. B **26**, 7867 (1982).
[33] G. Danan, A. Pinczuk, J. P. Valladares, L. N. Pfeiffer, K. W. West, and C. W. Tu, Phys. Rev. B **39**, 5512 (1989).